Erosion, fault initiation and topographic growth of the North Qilian Shan (northern Tibetan Plateau)

Dewen Zheng[1], Marin K. Clark[2], Peizhen Zhang[1], Wenjun Zheng[1], and Kenneth A. Farley[3]

[1]*State Key Laboratory of Earthquake Dynamics, Institute of Geology, China Earthquake Administration, Beijing 100029, China*
[2]*Department of Geological Sciences, University of Michigan, 1100 North University Avenue, Ann Arbor, Michigan 48105, USA*
[3]*Division of Geological and Planetary Sciences, California Institute of Technology, 1200 E. California Boulevard, Pasadena, California 91125, USA*

ABSTRACT

New apatite (U-Th)/He from the northeastern margin of the Tibetan Plateau (north Qilian Shan) indicate rapid cooling began at ~10 Ma, which is attributed to the onset of faulting and topographic growth. Preservation of the paleo-PRZ in the hanging wall and growth strata in the footwall allow us to calculate vertical and horizontal fault slip rates averaged over the last 10 Myr of ~0.5 mm/yr and ~1 mm/yr respectively, which are within a factor of two consistent with Holocene slip rates and geodetic data. Low fault slip rates since the initiation of the northern Qilian Shan fault suggest that total horizontal offset did not exceed 10 km. Further, emergence of the northern Qilian Shan occurs during a period of increased aridity in northern Tibet but is associated with only a minor expansion of the northern plateau perimeter, which is well established near collision time. Outgrowth of the northern Qilian Shan at ~10 Ma could be simple propagation of the larger Qilian Shan system, occurring in response to decreased slip rates on the Altyn Tagh fault or as a result of the change in GPE of the central plateau.

INTRODUCTION

The large size and youthfulness of the Tibetan orogen make it a prime location to study topographic growth, erosion and the effect of topography on climate. Mountain range exhumation histories and lithologic changes in basin stratigraphy in northeastern Tibet have been used as a proxy for the development of high mean elevations. However, pre-Cenozoic cooling ages from exhumed fault blocks and lack of precise age data in basin deposits make linkages between orogenesis, exhumation/sedimentation, and climate tentative (e.g., Metivier et al., 1998; Zheng et al., 2000; Jolivet et al., 2001; Fang et al., 2003).

The Qilian Shan lies along the northeastern margin of the Tibetan Plateau—a location where the initial timing of plateau growth is poorly known (Fig. 1). Thrust faulting in the Qilian Shan has been linked to crustal thickening and topographic growth, as well as to the accommodation of motion of the Altyn Tagh fault by the transfer of left-lateral strike-slip motion to oblique thrusting (Burchfiel et al., 1989; Peltzer et al., 1989; Meyer et al., 1998; Tapponnier et al., 1990). Previous suggestions for the onset time of Qilian Shan deformation, including that of the North Qaidam terrane, range from Paleocene to Pliocene time (Dupont-Nivet et al. 2004; Horton et al., 2004; Jolivet et al., 2001; Yin et al., 2002, 2008; George et al., 2001; Wang et al., 2004; Fang et al., 2004; Metivier et al., 1998). Analysis of Cenozoic stratigraphy in the western Hexi Corridor and adjacent north Qilian Shan range identifies facies changes in Miocene time related to range growth (Bovet et al., 2009). Growth strata within the dated section of the Niugetao Formation (~9 Ma) of the Jiuxi Basin (central Hexi Corridor) suggests fault activity of the North Qilian Shan thrust during late Miocene time (Fang et al., 2004), but does not constrain fault initiation or range growth. Cooling histories from fault bounded range blocks are well-suited for determining the initiation of faulting; however, previous apatite fission-track and $^{40}Ar/^{39}Ar$ dating in hanging wall rocks have

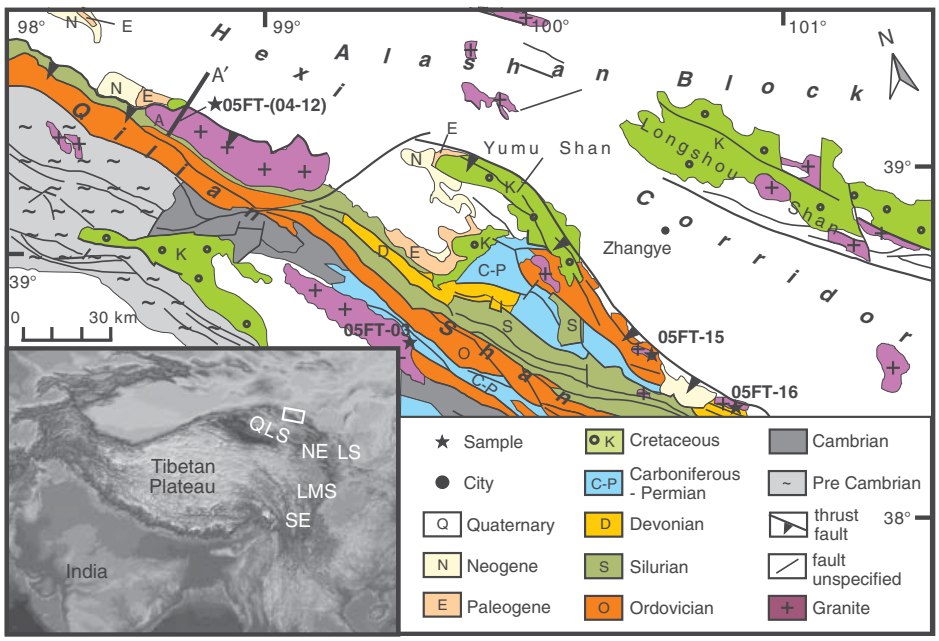

Figure 1. Sample location map. Cross-section line A-A′ shows location of profile in Figure 3. Inset map: QLS—Qilian Shan; LS—Liupan Shan; LMS—Longmen Shan; SE—southeastern Tibet; NE—northeastern Tibet.

Geosphere; December 2010; v. 6; no. 6; p. 937–941; doi: 10.1130/GES00523.1; 3 figures; 2 supplemental tables.

been unsuccessful in directly dating the onset of rapid cooling related to erosional exhumation of the range because with exception of a single sample, cooling ages are Mesozoic, which suggests that exhumation in response to Cenozoic thrust and reverse faulting has been insufficient to exhume completely reset ages (< 4–6 km) (Jolivet et al., 2001; George et al., 2001).

Apatite helium ages have a lower closure temperature than thermochronometric techniques previously applied in the Qilian Shan, and so potentially record a thermal history related to fault-induced erosional exhumation. Further, we discuss how the preservation of the paleo-partial retention zone (PRZ) for helium diffusion in hanging wall rocks can be utilized as a passive marker to determine subsequent fault motion. When syn-tectonic sediments are preserved in the footwall, the paleo-PRZ can be used to measure long-term geologic offsets where the appropriate stratigraphic markers in the hanging wall are absent, which is a common structural limitation in basement-cored structures (Clark and Bilham, 2008). Thus in circumstances where erosion is limited to a few kilometers, apatite helium ages provide constraints on both the initiation of faulting and fault offset, and Myr scale faulting rates can be determined.

GEOLOGIC SETTING AND SAMPLING STRATEGY

The Cenozoic tectonics of the Qilian Shan and adjacent Hexi Corridor are characterized by folding, thrust faulting, and strike-slip faulting that partially accommodate modern India-Eurasia plate convergence (Tapponnier et al., 1990; Yuan et al., 2004). Geodetic shortening rates are 5.5 (±1.5) mm/yr (Zhang et al., 2004) between the Qaidam and Alashan blocks, and active shortening deformation to the south is distributed throughout the ~270 km wide Qilian Shan plateau (Institute of Geology, 1993; Metivier et al., 1998; Yuan et al., 2004). The northernmost structure of the Qilian Shan, the North Qilian Shan Thrust, juxtaposes low-grade metamorphic lower Paleozoic rocks (slates, phyllites, limestones, volcanic, and granitic rocks) over Cenozoic sedimentary rocks in the Hexi Corridor basin (Gansu Geological Bureau, 1989; Fang et al., 2004).

The North Qilian Shan Thrust has formed a 2–3 km topographic escarpment above the Hexi Corridor basin. A coarsening-upward succession of lacustrine-fluvial deposits 2000–3000 m thick is preserved within the basin (Gansu Geological Bureau, 1989; Fang et al., 2004) and is dated to be mid-Oligocene to Quaternary depositional age based on paleontology (Bally et al., 1986; Wang and Coward, 1993) and magnetostratigraphy (Fang et al., 2004).

We dated 12 samples for (U-Th)/He thermochronometry that were collected from Paleozoic granites in the hanging wall of the North Qilian Shan Thrust (Fig. 1). Nine samples were collected on a ~1100 m vertical transect within a single pluton. These samples are used to identify changes in erosion rate that may be related to fault motion. Three additional samples were collected 100–200 km along strike to the east (Fig. 1). Although the density of sampling to the east is not great enough to determine if propagation of erosion occurred along strike of the fault, these samples provide some indication of how erosion magnitude may vary spatially and thus how regional a particular erosion history may be. Samples were analyzed for single-grain apatite (U-Th)/He ages using standard procedures at Caltech (Farley and Stockli, 2002), and sample mean ages are reported as the average of 3 or 4 individual grain analyses (Supplemental Tables 1[1] and 2[2]).

RESULTS

Apatite helium ages indicate the time at which the sample cooled through its closure isotherm or ~60 °C for this sample suite based on a radiation damage model for He diffusion kinetics (Farley, 2002; Shuster et al., 2006). Helium ages on the vertical transect increase with elevation with a distinct change in the apparent exhumation rate at ~2700 m. Below 2700 m elevation, analyses define a steep age/elevation gradient with an increase from 7.2 to 9.5 Ma. Above 2700 m analyses define a shallow age/elevation gradient, with ages increasing from 9.5 to 106 Ma and a pronounced change in age/elevation gradient at ~9.5 Ma (Fig. 2). Three samples collected ~200 km southeast of the vertical transect are shown on the same plot (gray) and yield Mesozoic ages at high elevation but younger ages at low elevations compared to the vertical transect (Fig. 2; Supplemental Table 1 [see footnote 1]). While these off-transect samples are too few to constrain a robust change in age/elevation gradient at a second location, these ages are generally consistent with a similar exhumation history along strike of the fault.

[1]Supplemental Table 1. Excel file of sample location and summary age data. If you are viewing the PDF of this paper or reading it offline, please visit http://dx.doi.org/10.1130/GES00523.S1 or the full-text article on www.gsapubs.org to view Supplemental Table 1.

[2]Supplemental Table 2. Excel file of (U-Th)/He replicate analyses. If you are viewing the PDF of this paper or reading it offline, please visit http://dx.doi.org/10.1130/GES00523.S2 or the full-text article on www.gsapubs.org to view Supplemental Table 2.

INTERPRETATION OF HELIUM AGES: TIMING OF FAULT INITIATION AND FAULT SLIP RATE

In a compressional tectonic setting, an abrupt increase in apparent exhumation rate on an age/elevation plot typically signals accelerated erosion most likely related to the upward motion of the hanging wall over the footwall (e.g., Wagner and Reimer, 1972; Wagner et al., 1977; Fitzgerald et al. 1995; Stockli et al., 2000; Reiners and Brandon, 2006). Ages that predate this transition define the base of the fossil helium partial retention zone prior to rapid exhumation, i.e., the "lower break in slope" on an age/elevation diagram and can therefore be used to reconstruct the relative elevation of the land surface prior to faulting (Clark and Bilham, 2008). Such a reconstruction provides a marker horizon in the hanging wall that can be used to determine relative motion across the fault and is particularly useful in geologic settings where stratigraphic markers are absent in the hanging wall. Because non-vertical pathways of rocks can complicate quantitative interpretation of erosion rate from age/elevation information alone (e.g., Huntington et al., 2007), we focus only on timing of abrupt change in apparent erosion rate. As described below, we derive fault slip rates from offset markers across the fault and initiation age of faulting, not from the apparent erosion rate recorded by age/elevation data.

Timing of Fault Motion

An abrupt increase in erosion rate in the hanging wall of a thrust or reverse fault likely signals fault activity and enhanced erosion at that time. The attribution of increased erosion rate to fault activity may be invalid if climate conditions caused enhanced erosion of pre-existing topography or delayed erosion following fault motion to a climate period of greater erosivity. However, ~9 Ma growth strata found at the base of the Niugetao Fm. in the Hexi Corridor represent the initiation of deposition related to fault motion (Yang et al., 2007; Fang et al., 2004) (Fig. 1). The correlation of growth strata with an increase in exhumation rate is strong evidence of synchronous fault motion and accelerated erosion.

Regional climate conditions were also unlikely to have caused the erosion signal we observe at ~10 Ma. Isotopic and lithostratigraphic evidence from basins across northern Tibet suggests arid conditions began in Oligocene time and is attributed to the retreat of the Paratethys epicontinental sea, global climate changes, or the early rise of mountain ranges in northern Tibet, which block moisture from the south and east (Wang et al., 2003; Graham

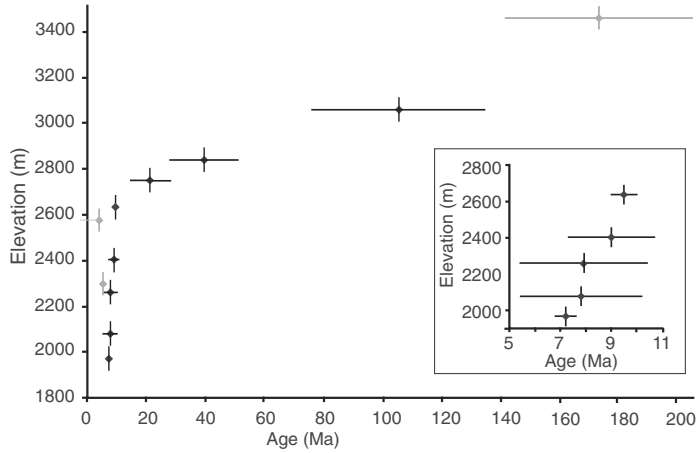

Figure 2. Age-elevation diagram. Black—mean (U-Th)/He ages for age/depth transect. Gray—mean (U-Th)/He ages for samples located along strike of the thrust, east of the vertical transect. Helium age uncertainties are calculated from the standard error of replicate analyses for individual samples (6–38% [2σ]). One sample (05FT-08) did not yield enough high quality apatite for a helium analysis.

et al., 2005; Dupont-Nivet et al., 2006). Climate proxies from Linxia Basin in northeastern Tibet suggest an increase in aridity at 12–13 Ma with the period of greatest aridity occurring between 9.6 and 8.5 Ma (Dettman et al., 2003; Fan et al., 2007). A Neogene increase in $\delta^{18}O$ values from sediments in the Tarim and Qaidam Basins may also represent a regional shift to more arid conditions (Kent-Corson et al., 2009), correlative with an increase in dust deposition in the North Pacific and an increase in loess deposition within northern China at 7–8 Ma (Rea et al., 1998; Sun et al., 1998).

Decreased precipitation would likely cause a decrease in climatically driven erosion rates, so climatic forcing at ca. 10 Ma is not likely to be the cause of the exhumation rate increase indicated by our data. Given the presence of synchronous growth strata and evidence for a lack of climate forcing, we attribute the increase in exhumation rate at ca. 10 Ma to fault initiation and the likely generation of steep topography of the northernmost escarpment of the modern Tibetan Plateau. Helium ages are 2–3 Myr younger at low elevations east of the vertical transect, which suggests that either faulting initiated a few million years later or higher erosion rates occur along strike assuming no warping of isotherms between the two sample collection sites.

Fault Slip Rate

Vertical separation of marker horizons across the fault, combined with the dip of the fault and age constraints, can be used to calculate long-term (Myr) vertical and horizontal fault slip rates. The base of the PRZ can be used to reconstruct the relative elevation of the ca. 10 Ma land surface (i.e., the land surface just prior to fault initiation with respect to the modern elevation of the PRZ) in the hanging wall (Fig. 3). This reconstruction provides a marker horizon in the hanging wall, which can be correlated across the fault in the footwall to the foreland basin stratigraphic horizon that represents the initial deposition at the onset of faulting identified from growth strata (Fig. 3) (i.e., Clark and Bilham, 2008). We discuss the relative offset of markers across the fault in terms of modern elevation for ease of discussion as we have no constraints on paleoelevation.

In order to calculate the closure isotherm depth, we first calculate the helium closure temperature based on an average eU (53 ppm) (Supplemental Table 2 [see footnote 2]) and an average cooling rate (4.5–9 °C/Myr) determined from the apparent exhumation rate of the interval of fast exhumation (0.3 mm/yr) (Fig. 2 inset) and a range of typical continental geothermal gradients (15–30 °C/km). Based on the radiation damage trapping model of Shuster et al., (2006), we determine a closure temperature of 58–62 °C. Using a surface temperature of 10 °C and a range of typical continental geothermal gradients (15–30 °C/km), we calculate an average closure isotherm depth of 2.6 ± 1 km.

The base of the fossil PRZ is located at 2700 m elevation (Fig. 2), and the ca. 10 Ma surface is reconstructed to 5.3 ± 1.0 km elevation based on the calculation of closure isotherm depth (Fig. 3). Growth strata formed at the base of the Niugetao Fm. (900 m depth beneath the surface or 600 m elevation) in the Hexi Corridor represent the initiation of deposition related to fault motion (Yang et al., 2007) and have been dated with magnetostratigraphy at ~9 Ma (Fang et al., 2004). Fault throw of 4.7 km is determined from the separation between the base of the Niugetao Fm. and the reconstructed ca. 10 Ma land surface in the hanging wall, and we assume faulting has been continuous since the onset time and thus the calculated rates reflect Myr scale average of fault motion (Fig. 3). Using estimates of fault throw (4.7 ± 1.0 km), fault initiation (9–10 Ma), and a fault dip (30°; Yang et al. 2007) that is assumed to remain unchanged in time, we calculate Myr time scale vertical and horizontal fault slip rates of ~0.5 mm/yr and ~1 mm/yr respectively, and a horizontal offset of 8.2 ± 1.8 km. Uncertainty

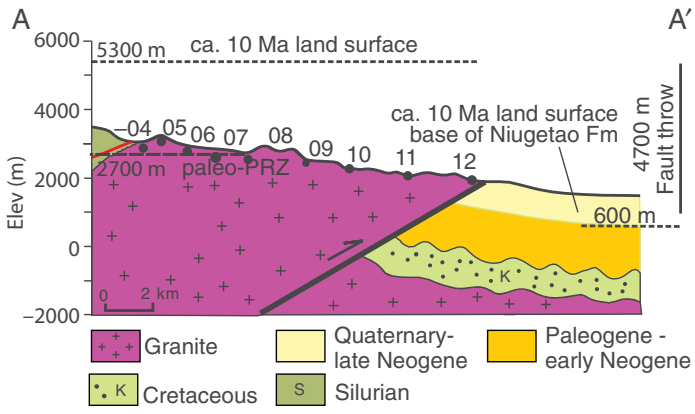

Figure 3. Structural offset across the North Qilian Shan thrust (NQT). Ca. 10 Ma land surface is reconstructed from the elevation of the fossil helium PRZ and correlated with the base of the Niugetao Fm in order to determine fault throw.

on the horizontal offset is likely to be underestimated because it includes only the uncertainty on the vertical offset and not the fault geometry. Changes in fault geometry at depth or through time would increase the uncertainty in the horizontal offset.

Fault slip rates averaged over the past ~10 Myr are consistent with late Pleistocene–Holocene rates determined in the Yumu Shan (vertical rates of 0.4–1.9 mm/yr) (Tapponnier et al., 1990) and for the Zhangye Thrust (0.6–0.9 mm/yr and 0.4–1.1 mm/yr vertical and horizontal rates, respectively), a correlative thrust ~100 km to the east (Hetzel et al. 2004). Ten million year rates are also broadly consistent with the average geodetic velocity (horizontal) (5.5 ± 1.5 mm/yr; Zhang et al., 2004) measured between the Qaidam and Alashan blocks assuming that deformation is distributed throughout the ~270 km wide Qilian Shan plateau (Institute of Geology, 1993; Metivier et al., 1998; Yuan et al., 2004). Low slip rates that were maintained over the past 10 million years imply that total horizontal fault offsets in the North Qilian range are likely to be small (< 10 km).

DISCUSSION

We interpret slow cooling of the northern Qilian Shan during 106–10 Ma as an indication that faulting did not reach this portion of the range until relatively late in the orogen's history. Fault initiation at ca. 10 Ma in the northern Qilian Shan range appears to be synchronous along strike for at least ~100 km (Bovet et al., 2009). Such a young age of faulting broadly conforms to the step-wise growth model of plateau formation (Tapponnier et al., 2001) only in the sense that northern Tibet represents the youngest or most recent stage of orogenisis. Unlike the step-wise model, we suggest that the late Miocene initiation of the northern Qilian Shan fault represents only a modest advancement of ~100 km of the plateau perimeter based on deformation ages in the central and southern parts of the range. Motion on the northern range front occurs significantly later than initial faulting in the central Qilian Shan (>33 Ma) (Yin et al., 2002), southern Qilian Shan/N. Qaidam terrane (broadly speaking since Paleocene time) (Yin et al., 2008) though locally faults initiate at later times (e.g., Sun et al., 2005; Wang et al., 2004), broad deformation in northeastern Tibet between 55 and 52 Ma (Dupont-Nivet et al., 2004; Horton et al., 2004) and locally along the West Qinling fault at 45–50 Ma (Clark et al., 2010). Late Miocene initiation of the north Qilian fault also significantly postdates the initial Oligocene motion along the Altyn Tagh fault (Ritts et al., 2004).

Miocene growth of the northern Qilian Shan could be local and simply represent the latest outgrowth of faulting within the larger Qilian Shan/N. Qaidam region in the direction of plate convergence. As Bovet et al. (2009) note, Miocene growth of the northern Qilian Shan also follows a decrease in fault slip accumulation of the Altyn Tagh fault (post-early Miocene; Yue et al., 2004) and uplift of the Altun Shan and SE Tarim Basin since 15–16 Ma (Ritts et al., 2008). Therefore between early to middle Miocene time, the kinematics of the Altyn Tagh fault system in northern Tibet may have evolved from fast strike-slip motion to distributed uplift and reverse faulting (Ritts et al., 2008). Following this change from strike-slip to shortening, the northern plateau margin expands to the northern Qilian Shan by 10 Ma, which may represent the final stage of distributed, reverse faulting and range growth that follows in the wake of decreased slip along the Altyn Tagh fault.

Alternatively, or in concert with the aforementioned changes to the Altyn Tagh fault system, convective removal of an overthickened, gravitationally unstable mantle lithosphere beneath north-central Tibet with associated elevation gain of 1–2 km of the central plateau (Molnar et al., 1993) would augment the force per unit length that Tibet applies to its surroundings, perhaps sufficiently to displace northward the Qaidam Basin as an effectively rigid block. The thinner and less deformed crust of the Qaidam Basin may act as a rigid block capable of deforming the region to the east or north by rotation or northward propagation (Dupont-Nivet et al., 2002). Increased topographic gradients may cause compressional stresses that translate the Qaidam Basin northward as a secondary indenter that causes deformation of the Qilian Shan to step northward and faulting in northeastern Tibet to extend eastward to the Liupan Shan (Zheng et al., 2006).

Since 10 Ma, the northeastern perimeter of the Tibetan Plateau advanced for nearly the first time since collision began, but it is important to note that the magnitude of this change was small compared to the north-south extent of the plateau prior to 10 Ma. Faulting within the central and southern Qilian Shan and in northeastern Tibet begins near the time of Indo-Asian collision (Dupont-Nivet et al., 2004; Horton et al., 2004; Yin et al., 2008; Clark et al., 2010). In late Miocene time, the areal extent of faulting expands northward by ~100 km from the central to the northern Qilian Shan and eastward by ~200 km to the Liupan Shan (at ~8 Ma; Zheng et al., 2006) (Fig. 1 inset). Such a modest expansion in northern Tibet can be correlated with the more dramatic development of the eastern plateau by lower crustal flow, where more than 2.25×10^7 km^3 crustal volume has been added east of the main collision zone (Royden et al., 1997; Clark and Royden, 2000; Clark et al., 2005a) since mid-late Miocene time (Kirby et al., 2002; Clark et al., 2005b; Ouimet et al., 2010). This suggests that the late Miocene to recent period of plateau growth was mainly east, and not north as might be simply predicted from plate boundary stresses applied by the northward motion of India.

ACKNOWLEDGMENTS

We thank Lindsey Hedges, Alison Duvall, Peter Molnar, and support by the National Science Foundation of China (40672134 and 40234040), and DFIGCEA0607122, and the US National Science Foundation, Continental Dynamics Program (EAR-0507431). Reviews by G. Dupont-Nivet, A. Carter, K. Huntington, and three anonymous reviewers improved the clarity of this manuscript.

REFERENCES CITED

Bally, A.W., Chou, I.M., Clayton, R., Eugster, H.P., Kidwell, S., Meckel, L.D., Ryder, R.T., Watts, A.B., and Wilson, A.A., 1986, Notes on sedimentary basins in China–Report of the American sedimentary basins delegation to the People's Republic of China: U.S. Geological Survey Open File Report 86-327, 108 p.

Bovet, P.M., Ritts, B.D., Gehrels, G., Abbink, A.O., Darby, B., and Hourigan, J., 2009, Evidence of Miocene crustal shortening in the northern Qilian Shan from Cenozoic stratigraphy of the western Hexi Corridor, Gansu Province, China: American Journal of Science, v. 309, p. 290–329, doi: 10.2475/00.4009.02.

Burchfiel, B.C., Deng, Q.D., Molnar, P., Royden, L., Wang, Y.P., Zhang, P.Z., and Zhang, W., 1989, Intracrustal detachment with zones of continental deformation: Geology, v. 17, p. 748–752, doi: 10.1130/0091-7613(1989)017<0448:IDWZOC>2.3.CO;2.

Clark, M.K., and Bilham, R., 2008, Miocene rise of the Shillong Plateau and the beginning of the end for the Eastern Himalaya: Earth and Planetary Science Letters, v. 269, no. 3-4, p. 337–351, doi: 10.1016/j.epsl.2008.01.045.

Clark, M.K., Farley, K.A., Zheng, D., Wang, Z., and Duvall, A., 2010, Early Cenozoic faulting of the northern Tibetan Plateau margin from apatite (U-Th)/He ages: Earth and Planetary Science Letters, v. 296, p. 78–88, doi:10.1016/j.epsl.2010.04.051.

Clark, M.K., Bush, J.W.M., and Royden, L.H., 2005a, Dynamic topography produced by lower crustal flow against rheologic strength heterogeneities bordering the Tibetan Plateau: Geophys. J. Int., v. 162, p. 575–590, doi:10.1111/j.1365246X.2005.02580.x.

Clark, M.K., House, M.A., Royden, L.H., Whipple, K.X., Burchfiel, B.C., Zhang, X., and Tang, W., 2005b, Late Cenozoic uplift of the southeastern Tibet: Geology, v. 33, no. 6, p. 525–528, doi: 10.1130/G21265.1.

Clark, M.K., and Royden, L.H., 2000, Topographic ooze: Building the eastern margin of Tibet by lower crustal flow: Geology, v. 28, no. 8, p. 703–706, doi: 10.1130/0091-7613(2000)28<703:TOBTEM>2.0.CO;2.

Dettman, D.L., Fang, X., Garzione, C.N., and Li, J., 2003, Uplift-driven climate change at 12 Ma: A long $\delta^{18}O$ record from the NE margin of the Tibetan plateau: Earth and Planetary Science Letters, v. 214, p. 267–277, doi: 10.1016/S0012-821X(03)00383-2.

Dupont-Nivet, G., Butler, R., Yin, A., and Chen, X., 2002, Paleomagnetism indicates no Neogene rotation of the Qaidam Basin in northern Tibet during the Indo-Asian collision: Geology, v. 30, no. 3, p. 263–266, doi: 10.1130/0091-7613(2002)030<0263:PINNRO>2.0.CO;2.

Dupont-Nivet, G., Horton, B.K., Butler, R.F., Wang, J., Zhou, J., and Waanders, G.L., 2004, Paleogene clockwise tectonic rotation of the Xining-Lanzhou region, northeastern

Tibetan Plateau: Journal of Geophysical Research, v. 109, p. B04401, doi: 10.1029/2003JB002620.

Dupont-Nivet, G., Krijgsman, W., Langereis, C.G., Abels, H.A., Dai, S., and Fang, X., 2006, Tibetan Plateau aridification linked to global cooling at the Eocene-Oligocene transition: Nature, v. 445, p. 635–638, doi: 10.1038/nature05516.

Fan, M.J., Dettman, D.L., Song, C.H., and Fang, X.M., 2007, Climatic variation in the Linxia basin, NE Tibetan Plateau from 13.1 to 4.3 Ma: The stable isotope record: Palaeogeography, Palaeoclimatology, Palaeoecology, v. 247, p. 313–328, doi: 10.1016/j.palaeo.2006.11.001.

Fang, X., Garzione, C., Van der Voo, R., Li, J., and Fan, M., 2003, Flexural subsidence by 29 Ma on the NE edge of Tibet from the magnetostratigraphy of Linxia Basin, China: Earth and Planetary Science Letters, v. 210, p. 545–560, doi: 10.1016/S0012-821X(03)00142-0.

Fang, X., Zhao, Z., Li, J., Yan, M., Pan, B., Song, C., and Dai, S., 2004, Paleomagnetism of the late Cenozoic stratigraphy in the Jiuxi Basin north of the Qilian Mts. and uplift the Tibetan Plateau: Science in China (D), v. 34, p. 97–106.

Farley, K.A., 2002, (U-Th)/He dating: Techniques, calibrations, and applications, *in* Noble Gases in Geochemistry and Cosmochemistry: Reviews in Mineralogy and Geochemistry, v. 47, p. 819–844, doi: 10.2138/rmg.2002.47.18.

Farley, K.A., and Stockli, D.F., 2002, (U-Th)/He dating of phosphates: Apatite, monazite, and xenotime, *in* Phosphates: Geochemical, geobiological, and materials importance: Reviews in Mineralogy and Geochemistry, v. 48, p. 559–577, doi: 10.2138/rmg.2002.48.15.

Fitzgerald, P.G., Sorkhabi, R.B., and Redfield, T.F., 1995, Uplift and denudation of the central Alaska range: A case study in the use of apatite fission-track thermochronology to determine absolute uplift parameters: Journal of Geophysical Research, v. 100, p. 20,175–20,191, doi: 10.1029/95JB02150.

Gansu Geological Bureau, 1989, Regional geology of Gansu Province: Beijing, Geological publishing house, 692 p. (in Chinese).

George, A.D., Marshallsea, S.J., Wyrwoll, K.H., Chen, J., and Lu, Y., 2001, Miocene cooling in the northern Qilianshan, northeastern margin of the Tibetan plateau, revealed by apatite fission-track and vitrinite- reflectance analysis: Geology, v. 29, p. 939–942.

Graham, S.A., Chamberlain, C.P., Yue, Y., Ritts, B., Hanson, A.D., Horton, T.W., Waldbauer, J.R., Poage, M.A., and Feng, X., 2005, Stable isotope records of Cenozoic climate and topography: Tibetan Plateau and Tarim Basin: American Journal of Science, v. 305, p. 101–118.

Hetzel, R., Tao, M., Stokes, S., Niedermann, S., Ivy-Ochs, S., Switzerland, Z., Gao, B., Strecker, M.R., and Kubik, P.W., 2004, Late Pleistocene/Holocene slip rate of the Zhangye thrust (Qilian Shan, China) and implications for the active growth of the northeastern Tibetan Plateau: Tectonics, v. 23, doi: 10.1029/2004TC001653.

Horton, B.K., Dupont-Nivet, G., Zhou, J., Waanders, G.L., Butler, R.F., and Wang, J., 2004, Mesozoic-Cenozoic evolution of the Xining-Minhe and Dangchang basins, northeastern Tibetan Plateau: Journal of Geophysical Research, v. 109, p. B04401, doi: 10.1029/2003JB002620.

Huntington, K.W., Ehlers, T.A., Hodges, K.V., and Whipp, D.M., 2007, Topography, exhumation pathway, age uncertainties, and the interpretation of thermochronometer data: Tectonics, v. 26, p. TC4012, doi: 10.1029/2007TC002108.

Institute of Geology, China Seismological Bureau and Lanzhou Institute of Seismology, 1993, The Qilian mountain-Hexi Corridor active fault system: Beijing, Seismological Press, 340 p. (in Chinese).

Jolivet, M., Brunel, M., Seward, D., Xu, Z., Yang, J., Roger, F., Tapponnier, P., Malavieille, J., Arnaud, N., and Wu, C., 2001, Mesozoic and Cenozoic tectonics of the northern edge of the Tibetan plateau: fission-track constraints: Tectonophysics, v. 343, p. 111–134, doi: 10.1016/S0040-1951(01)00196-2.

Kent-Corson, M., Ritts, B.D., Zhuang, G., Bovet, P.M., Graham, S.A., and Chamberlain, C.P., 2009, Stable isotopic constraints on the tectonic, topographic, and climatic evolution of the northern margin of the Tibetan Plateau: Earth and Planetary Science Letters, doi: 10.1016/j.epsl.2009.03.011.

Kirby, E., Reiners, P.W., Krol, M.A., Whipple, K.X., Hodges, K.V., Farley, K.A., Tang, W., and Chen, Z., 2002, Late Cenozoic evolution of the eastern margin of the Tibetan Plateau: Inferences from $^{40}Ar/^{39}Ar$ and (U-Th)/He thermochronology: Tectonics, v. 21, doi: 10.1029/2000TC001246.

Meyer, B., Tapponnier, P., Bourjot, L., Metivier, F., Gaudemer, Y., Peltzer, G., Shunmin, G., and Zhitai, C., 1998, Crustal thickening in Gasu-Qinghai, lithospheric mantle subduction, and oblique, strike-slip controlled growth of the Tibet plateau: Geophysical Journal International, v. 135, p. 1–47, doi: 10.1046/j.1365-246X.1998.00567.x.

Metivier, F., Gaudemer, Y., Tapponnier, P., and Meyer, B., 1998, Northeastward growth of the Tibet Plateau deduced from balanced reconstruction of two depositional areas: The Qaidam and Hexi Corridor basins, China: Tectonics, v. 17, p. 823–842, doi: 10.1029/98TC02764.

Molnar, P., England, P., and Martinod, J., 1993, Mantle dynamics, uplift of the Tibetan Plateau, and the Indian monsoon: Reviews of Geophysics, v. 31, p. 357–396, doi: 10.1029/93RG02030.

Ouimet, W., Whipple, K.X., Royden, L., Reiners, P., Hodges, K., and Pringle, M., 2010, Regional incision of the eastern margin of the Tibetan Plateau: Lithosphere, v. 2, no. 1, p. 50–63, doi: 10.1130/L57.1.

Peltzer, G., Tapponnier, P., and Armijo, R., 1989, Magnitude of late Quaternary left-lateral displacements along the northern edge of Tibet: Science, v. 246, p. 1285–1289, doi: 10.1126/science.246.4935.1285.

Rea, D.K., Snoeckx, H., and Joseph, L.H., 1998, Late Cenozoic eolian deposition in the North Pacific: Asian drying, Tibetan uplift, and cooling of the northern hemisphere: Paleoceanography, v. 13, no. 3, p. 215–224, doi: 10.1029/98PA00123.

Reiners, P.W., and Brandon, M.T., 2006, Using thermochronology to understand orogenic erosion: Annual Review of Earth and Planetary Sciences, v. 34, p. 419–466, doi: 10.1146/annurev.earth.34.031405.125202.

Ritts, B.D., Yue, Y., and Graham, S.A., 2004, Oligocene-Miocene Tectonics and Sedimenation along the Altyn Tagh Fault, Northern Tibetan Plateau: Analysis of the Xorkol, Subei, and Aksay Basins: The Journal of Geology, v. 112, p. 207–229, doi: 10.1086/381658.

Ritts, B.D., Yue, Y., Graham, S.A., Sobel, E.R., Abbink, O.A., and Stockli, D., 2008, From sea level to high elevation in 15 million years: Uplift history of the northern Tibetan Plateau margin in the Altun Shan: American Journal of Science, v. 308, p. 657–678, doi: 10.2475/05.2008.01.

Royden, L.H., Burchfiel, B.C., King, R.W., Wang, E., Chen, Z., Shen, F., and Liu, Y., 1997, Surface Deformation and Lower Crustal Flow in Eastern Tibet: Science, v. 276, p. 788–790, doi: 10.1126/science.276.5313.788.

Shuster, D.L., Flowers, R.M., and Farley, K.A., 2006, The influence of natural radiation damage on helium diffusion kinetics in apatite: Earth and Planetary Science Letters, v. 249, p. 148–161, doi: 10.1016/j.epsl.2006.07.028.

Stockli, D.F., Farley, K.A., and Dumitru, T.A., 2000, Calibration of the apatite (U-Th)/He thermochronometer on an exhumed fault block, White Mountains: California Geology, v. 28, no. 11, p. 983–986.

Sun, D., Shaw, J., An, Z., Cheng, M., and Yue, L., 1998, Magnetostratigraphy and paleoclimatic interpretation of a continuous 7.2 Ma late Cenozoic aeolian sediment from the Chinese loess plateau: Geophysical Research Letters, v. 25, p. 85–88, doi: 10.1029/97GL03353.

Sun, Z.M., Yang, Z.Y., Pei, J.L., Ge, X., Wang, X., Yang, T., Li, W., and Yuan, S., 2005, Magnetostratigraphy of Paleogene sediments from northern Qaidam basin, China: implications for tectonic uplift and block rotation in northern Tibetan plateau: Earth and Planetary Science Letters, v. 237, p. 635–646, doi: 10.1016/j.epsl.2005.07.007.

Tapponnier, P., Meyer, B., Avouac, J.P., Peltzer, G., Gaudemer, Y., Guo, S.M., Xiang, H.F., Yin, K.L., Chen, Z.T., Cai, S.H., and Dai, H.G., 1990, Active thrusting and folding in the Qilian Shan, and decoupling between upper crust and mantle in northeastern Tibet: Earth and Planetary Science Letters, v. 97, no. 3–4, p. 382–403, doi: 10.1016/0012-821X(90)90053-Z.

Tapponnier, P., Xu, Z.Q., Roger, F., Meyer, B., and Arnaud, N., Wittlinger, G., Yang, J.S., 2001, Oblique stepwise rise and growth of the Tibet Plateau: Science, v. 294, p. 1671–1677.

Wagner, G.A., and Reimer, G.M., 1972, Fission-track tectonics: The tectonic interpretation of fission trace ages: Earth and Planetary Science Letters, v. 14, p. 263–268, doi: 10.1016/0012-821X(72)90018-0.

Wagner, G.A., Reimer, G.M., and Jäger, E., 1977, Cooling ages derived by apatite fission track, mica Rb-Sr, and K-Ar dating: The uplift and cooling history of the central Alps: Mem. Inst. Geol. Mineral. Univ. Padova, v. 30, p. 1–27.

Wang, F., Lo, C-H., Li, Q., Yeh, M-W., Wan, J., Zheng, D., and Wang, E., 2004, Onset timing of significant unroofing around Qaidam basin, northern Tibet, China: Constraints from $^{40}Ar/^{39}Ar$ and FT thermochronometry on granitoids: J. Asian Earth Sci., v. 24, p. 59–69, doi: 10.1016.j.jseaes.2003.07.004.

Wang, Q.M., and Coward, M.P., 1993, The Jiuxi basin, Hexi corridor, NW China: foreland structural features and hydrocarbon potential: Journal of Petroleum Geology, v. 16, p. 169–182, doi: 10.1111/j.1747-5457.1993.tb00104.x.

Wang, X., Wang, B., Qiu, Z., Xie, G., Xie, J., Downs, W., Qiu, Z., and Deng, T., 2003, Danghe area (western Gansu, China) biostratigraphy and implications in depositional history and tectonics of northern Tibetan Plateau: Earth and Planetary Science Letters, v. 208, p. 253–269, doi: 10.1016/S0012-821X(03)00047-5.

Yang, S., Cheng, X., Xiao, A., Chen, J., Fan, M., and Tain, D., 2007, The structural characteristics of Northern Qilian Shan Mountain Thrust Belt and its control on the oil and gas accumulation: Beijing, Science Press, p. 70–82 (in Chinese).

Yin, A., Rumelhart, P.E., Butler, R., Cowgill, E., Harrison, T.M., Foster, D.A., Ingersoll, R.V., Zhang, Q., Zhou, X., Wang, X., Hanson, A., and Raza, A., 2002, Tectonic history of the Altyn Tagh fault system in northern Tibet inferred from Cenozoic sedimentation: Geological Society of America Bulletin, v. 114, p. 1257–1295, doi: 10.1130/0016-7606(2002)114<1257:THOTAT>2.0.CO;2.

Yin, A., Dang, Y., Wang, L., Jiang, W., Chen, X., Gehrels, G.E., and McRivette, M.W., 2008, Cenozoic tectonic evolution of Qaidam basin and its surrounding regions (Part 1): The southern Qilian Shan-Nan Shan thrust belt and northern Qaidam basin: Geol. Soc. Am. Bull., v. 120, p. 813–846, doi:10.1130.B26180.1.

Yuan, D., Zhang, P., Liu, B., Gan, W., Mao, F., Wang, Z., Zheng, D., and Guo, H., 2004, Geometrical imagery and tectonic transformation of late Quaternary active tectonics in northeastern margin of Qinghai-Xizang Plateau: Acta Geologica Sinica, v. 78, p. 270–278.

Yue, Y., Ritts, B. D., Graham, S. A., Wooden, J. L., Gehrels, G. E., and Zhang, Z., 2004, Slowing extrusion tectonics: Lowered estimate of post-Early Miocene slip rate for Altyn Tagh fault: Earth Planet. Sci. Lett., v. 217, p. 111–122, doi:10.1016/S0012-821X(03)00544-2.

Zhang, P., Shen, Z., Burgman, R., Molnar, P., Wang, Q., Niu, Z., Sun, J., Wu, J., Sun, H., and You, X., 2004, Continuous deformation of the Tibetan Plateau constrained from Global Positioning measurements: Geology, v.32, p. 809–812.

Zheng, H.B., Powell, C.M., An, Z.S., Zhou, J., and Dong, D.R., 2000, Pliocene uplift of the northern Tibetan Plateau: Geology, v. 28, no. 8, p. 715–718, doi: 10.1130/0091-7613(2000)28<715:PUOTNT>2.0.CO;2.

Zheng, D., Zhang, P.-Zh., Wan, J., Yuan, D., Li, C., Yin, G., Zhang, G., Wang, Z., Min, W., and Chen, J., 2006, Rapid exhumation at ~8 Ma on the Liupan Shan thrust fault from apatite fission-track thermochronology: Implications for growth of the northeastern Tibetan Plateau margin: Earth and Planetary Science Letters, v. 248, p. 183–193, doi: 10.1016/j.epsl.2006.05.023.

Manuscript Received 12 May 2009
Revised Manuscript Received 9 April 2010
Manuscript Accepted 11 May 2010